Journal of Applied Sciences

ISSN 1812-5654

science alert

ANSInet
an open access publisher
http://ansinet.com

Journal of Applied Sciences 9 (1): 178-182, 2009
ISSN 1812-5654

Theoretical Study and Finite Element Simulation of Tearing in Hydroforming Process

S.A. Zahedi, A. Shamsi, A. Gorji, S.J. Hosseinipour and M. Bakhshi-Jouybari
Faculty of Mechanical Engineering, Babol University of Technology, P.O. Box 484, Babol, Iran

Abstract: An axisymmetric analysis was developed to investigate the tearing phenomenon in cylindrical Hydroforming Deep Drawing (HDD). By theoretical and finite element simulation methods, the critical fluid pressures which result rupture in the workpiece were studied. The results showed that the theoretical pressure path is an upper limit of the tearing path. The effects of anisotropy, drawing ratio, sheet thickness and strain hardening exponent on tearing diagram were also investigated. It is shown that die profile radius is effective on blank profile radius.

Key words: Hydroforming deep drawing, pressure path, axisymmetric analysis, finite element simulation, die profile radius, blank profile radius

INTRODUCTION

Hydroforming Deep Drawing (HDD) is one of the metal forming processes that is used in industry to produce complex sheets with high Limiting Drawing Ratio (LDR). Schematic of cylindrical cup drawing with HDD process is shown in Fig. 1. A pressurized fluid is employed in front of the workpiece. As the punch travels, the workpiece begins to deform into a cylindrical cup (Kandil, 2003).

Some of the advantages of sheet hydroforming are, improving the material formability, reduction of friction force, the accuracy of the forming part and the reduction of forming stages because of improvement of Limiting Drawing Ratio (LDR) (Soo-Ik *et al*., 2006; Parsa and Darbandi, 2008; Lang *et al*., 2005a).

Analysis of tearing phenomenon in hydroforming was studied by Zhang *et al*. (2000), Lang *et al*. (2005b) and Dachang *et al*. (2005). Generally, two kinds of material failure caused by inappropriate fluid pressure were identified. The failure by wrinkling at the lip area (The area that the blank is in contact with die and blank holder) results from insufficient fluid pressure and the failure by rupture on the top of the cup results from excessive fluid pressure (Sy-wei Lo *et al*., 1993).

Numerous researchers have attempted to explain theoretically the critical condition of rupture in hydroforming processes. Yossifon and Tirosh (1985), Tirosh and Hazut (1989) and Yossifon and Tirosh (1991) predicted rupture by using the criterion of plane strain failure and wrinkling instability by energy method. They also obtained tearing and wrinkling

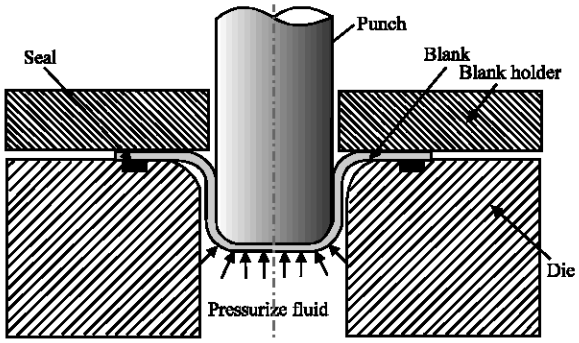

Fig. 1: Hydroforming Deep Drawing (HDD) process

diagrams for a die with radial pressure. Sy-wei Lo *et al*. (1993) extended the results of Yossifon and Tirosh (1991) for hemispherical cups. Wu *et al*. (2004) and Khandeparkar and Liewald (2008) obtained rupture and wrinkling diagrams for stepped punches by finite element simulation and experiments. Thiruvarudchelvan and Tan (2006) performed theoretical analysis and experimental approach from hydraulic pressure-assisted deep drawing process. Hama *et al*. (2007) developed an elasto-plastic finite element method for the sheet hydroforming of elliptical cups.

In this study, a suitable punch-stroke pressure path was obtained theoretically that avoids rupture in HDD process. Also, using the finite element simulation, the limiting pressure path was obtained. The results obtained showed that the theoretical pressure path is an upper limit of the tearing diagram.

This study was conducted in Babol university of technology in Iran country in 2007-2008 years.

Corresponding Author: M. Bakhshi-Jouybari, Faculty of Mechanical Engineering, Babol University of Technology, P.O. Box 484, Babol, Iran Tel/Fax: +98-111-3234205

BASIC THEORETICAL FORMULATIONS

A number of assumptions are made in this analysis that are:

- The thickness of the workpiece remains constant through out the process
- The principal strain axes do not rotate
- The tresca yield criterion is satisfied and the fluid pressure p is smaller than the radial stress σ_r and the tangential stress σ_θ. This assumption yields σ_r-σ_θ = σ_e.

For axisymmetric problems the polar equilibrium equation in the rim area is (Tirosh and Hazut, 1989):

$$\frac{d}{dr}(t\sigma_r)+\frac{t}{r}(\sigma_r-\sigma_\theta)+f(p)=0 \quad (1)$$

where, f (p) is the friction force in the rim area. By using the tresca criterion and a power law for the material properties, Eq. 1 can be rewritten as:

$$\frac{d}{dr}(t\sigma_r)+\frac{t}{r}(\sigma_0(\varepsilon_e)^n)+f(p)=0 \quad (2)$$

By using the normal anisotropy of the material in the formulation, the equivalent strain rate is denoted as:

$$\varepsilon_e^{\bullet}=\frac{1+R}{\sqrt{1+2R}}[\varepsilon_r^{\bullet 2}+(\frac{2R}{1+R})\varepsilon_r^{\bullet}\varepsilon_\theta^{\bullet}+\varepsilon_\theta^{\bullet 2}]^{\frac{1}{2}} \quad (3)$$

Since it was assumed that the axis of strain does not rotate and by considering that the material follows volume constancy in the plastic deformation, the effective strain ε_e is obtained by integrating Eq. 3:

$$\varepsilon_e=\sqrt{R_e}\varepsilon_r \quad (4)$$

By substituting Eq. 4 into Eq. 2, we have:

$$\frac{d}{dr}(t\sigma_r)+\frac{t}{r}(\sigma_0(R_e)^{\frac{n}{2}}\varepsilon_r^n)+f(p)=0 \quad (5)$$

Referring to Fig. 2 and substituting Eq. 5 for tension in area 1 we have:

$$\sigma_r^{(1)}+\int_{r_0}^{r}\frac{\sigma_0(R_e)^{n/2}(\varepsilon_r^{(1)})^n}{r}dr+\int_r^b\frac{f(p)}{t}dr=0 \quad (6)$$

By simplifying Eq. 6 for $\sigma_r^{(1)}$ we have:

$$\sigma_r^{(1)}=\int_r^b\frac{\sigma_0(R_e)^{n/2}(\varepsilon_r^{(1)})^n}{r}dr+\int_r^b\frac{f(p)}{t}dr \quad (7)$$

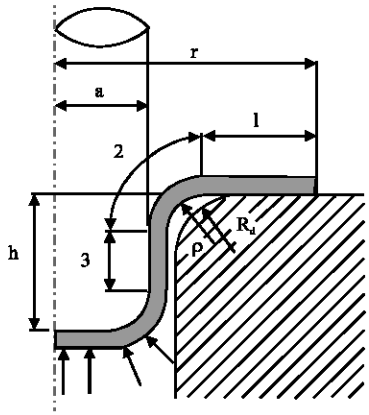

Fig. 2: Cylindrical sheet hydroforming process

The value of strain in area 1 is obtained by:

$$\varepsilon_r^{(1)}=\ln(\frac{G(r,h,p)}{r}) \quad (8)$$

Where:

$$G(r,h,p)=a\left\{1+(\frac{r}{a})^2-(1+\frac{\rho}{a})^2+\pi\frac{\rho}{a}(1+\frac{\rho}{a})-2(\frac{\rho}{a})^2+2(\frac{h}{a}-\frac{\rho}{a})Hv_{(\frac{h}{a}-\frac{\rho}{a})}\right\}^{\frac{1}{2}} \quad (9)$$

Here,

$$Hv_{(\frac{h}{a}-\frac{\rho}{a})}$$

is heaviside unit function. In the same manner, the stress in area 2 is as follows:

$$\sigma_r^{(2)}=\sigma_{r\,(r=a+\rho)}^{(1)}+\int_r^{a+\rho}\frac{\sigma_0(\varepsilon_r^{(2)})^nR_e^{n/2}}{r}dr \quad (10)$$

in which the strain in area 2, $\varepsilon_r^{(2)}$, is:

$$\varepsilon_r^{(2)}=\ln(\frac{F(r,h,p)}{r}) \quad (11)$$

Where:

$$F(r,h,p)=a\left\{1+2\frac{\rho}{a}(1+\frac{\rho}{a})(\frac{\pi}{2}-\beta)-2(\frac{\rho}{a})^2\cos\beta+2(\frac{h}{a}-\frac{\rho}{a})Hv_{(\frac{h}{a}-\frac{\rho}{a})}\right\}^{\frac{1}{2}} \quad (12)$$

In Eq. 12, β is an angle shown in Fig. 3 and is obtained by:

$$\beta=\sin^{-1}(\frac{a+\rho-r}{\rho}) \quad (13)$$

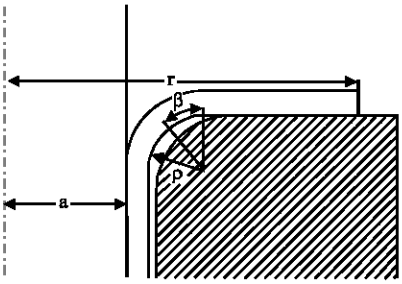

Fig. 3: Geometry of β angle in analytical equations

If the bending stress is neglected and the radial stress σ_r is calculated for the pure radial drawing case, equilibrium of area (2) become:

$$\sigma_r^{(2)}(2\pi at) = P\pi[(a+\rho)^2 - (a)^2] \quad (14)$$

ANALYSIS OF TEARING IN HYDROFORMING DEEP DRAWING

Tearing occurred at the upper part of the punch; just at the beginning of draw workpiece. It is cause by the firm contact between the workpiece and punch due to circumferential compressive fluid pressure (Yossifon and Tirosh, 1985). This area is the transition between regions 2 and 3.The rate of tangential strain at the wall of the punch is zero. It mines:

$$\varepsilon_\theta^{\bullet} = 0 \quad (15)$$

By combining Eq. 15 and 3 and solving, then we have:

$$d\varepsilon_e^{(3)} = Zd\varepsilon_r^{(3)} \quad (16)$$

Yossifon and Tirosh (1985) predicted the instability of anisotropic material under biaxial plane strain conditions as fallows:

$$\frac{d\sigma_z}{d\varepsilon_e} = \frac{\sigma_e}{Z} \quad (17)$$

Where:

$$Z = \frac{(1+R)}{\sqrt{(1+2R)}} \quad (18)$$

So, if Eq. 17 is in Eq. 10 will have:

$$\sigma_{r\,critical} = \sigma_0 n^n Z^{n+1} \quad (19)$$

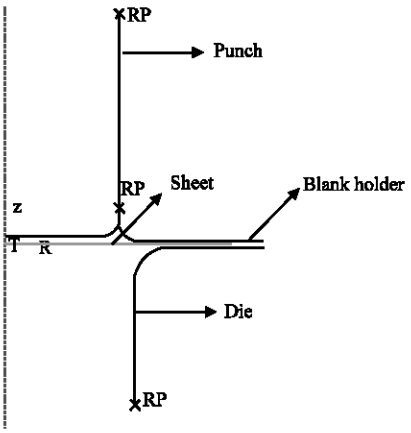

Fig. 4: The finite element model for the analysis of HDD in Abaqus software

Obviously, necking and rupture occur when the radial load reaches a maximum value.

$$F_{max} = \sigma_r^{(3)}(r=a)t \quad (20)$$

By equating Eq. 10 and 19 we have:

$$\sigma_0 n^n Z^{n+1} = \sigma_{r\,(r=a+\rho)}^{(1)} + \int_r^{a+\rho} \frac{\sigma_0(\varepsilon_r^2)R_e^{n/2}}{r}dr \quad (21)$$

By considering Eq. 14 and 21 we can obtain the fluid pressure causing rupture in the workpiece.

FINITE ELEMENT SIMULATION

The commercial finite element software ABAQUS 6.6 was used for the simulation. The finite element model created in the software is shown in Fig. 4.

In the simulations, the tools (punch, pressure chamber components and blank holder) were considered as rigid, while the sheet was considered to be deformable material. Coulomb friction equation was used to model the frictional condition between the blank and the tools. Due to symmetry, only half of the die and blank cross-section were modeled. In order to model the liquid, a uniform pressure distribution was used to apply the fluid pressure directly to the blank on the die opening. To introduce the pressure into the software use subroutine, called Vd load in ABAQUS, was used. The punch, die and blank holder were meshed with RAX2 (2-node linear axisymmetric rigid link for use in axisymmetric planar geometries) and the blank was meshed with SAX1 (2-node linear axisymmetric thin or thick shell).

Table 1: Material properties of the finite element simulation

Material	St 14
Thickness, t (mm)	1
Poisson ratio	0.3
Young's modulus, E (GPa)	210
Density, ρ (kg m^{-3})	7800
Isotropy (R)	1

Table 2: Material processes of the finite element simulation

Punch diameter, a (mm)	35
Blank diameter, b (mm)	75
Friction coefficient (μ)	0.08
strain hardening exponent (n)	0.27
σ_0 (MPa)	625

In order to define the rupture diagram, several counter pressure-punch displacement were prescribed for the simulation. The rupture criterion used in this paper is the critical effective strain at instability (Yossifon and Tirosh, 1985), as:

$$\varepsilon_{cr} = nz \tag{22}$$

$$z = \frac{1+R}{(1+2R)^{\frac{1}{2}}} \tag{23}$$

The material properties and the process parameters are given in Table 1 and 2, respectively.

RESULTS AND DISCUSSION

The tearing diagrams obtained by the analytical and finite element simulation are shown in Fig. 5.

Both of the methods suggested that a counter-pressure history with a somewhat smaller pressurization at the initial stage and a larger one at the later stage would normally result in a proper cylindrical cup product. As you see, the finite element simulation predicts limited zone compared with analytical equation. It means that analytical path is an upper limit to the tear diagram. Figure 6 investigates the effects of anisotropy, drawing ratio, sheet thickness and strain hardening component on tearing diagram.

In HDD the die radius does not always coincide the blank profile radius. The blank may move with variable contact with the die radius when counter-pressure going up so different values of blank profile radii obtained in HDD process for different die profile radii. This variation is shown in Fig. 7.

As it is see in Fig. 8, when the die profile radius is less than 2 mm the blank profile radius coincides the die curvature. But by growing die profile radii the blank profile radius changes along HDD process. Figure 8 has shown schematically this phenomenon.

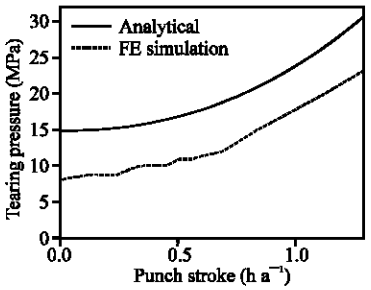

Fig. 5: Tearing diagram obtained from analytical approach and finite element simulation

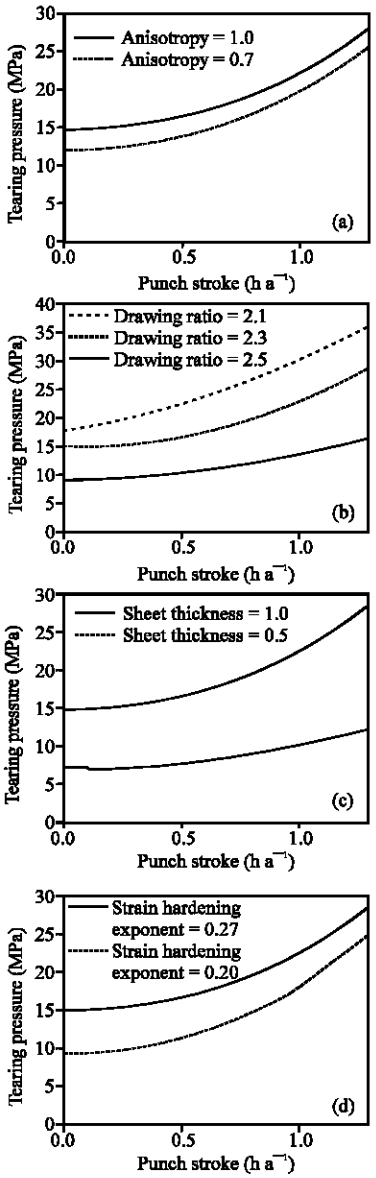

Fig. 6: Effect of, (a) Anisotropy, (b) Drawing ratio, (c) Sheet thickness and (d) Strain hardening component, on tearing diagram in HDD process

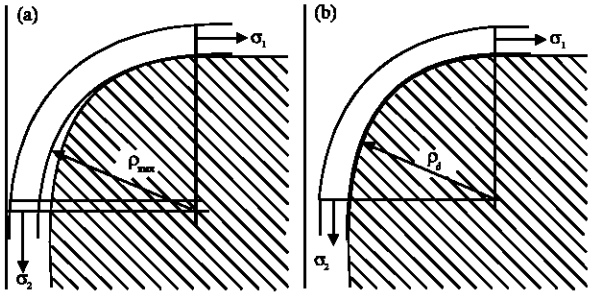

Fig. 7: Schematic of blank profile radius die profile radius, (a) R_d>2 and (b) R_d = 1

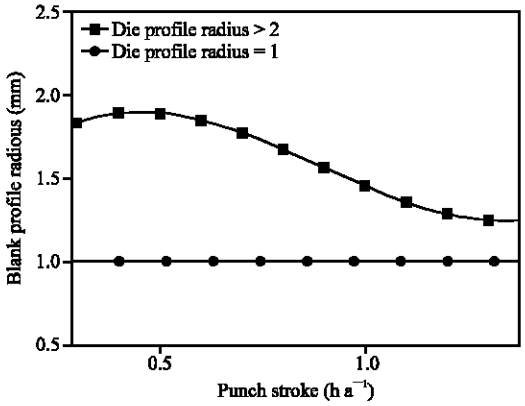

Fig. 8: Blank profile radius in HDD process for different dies curvature

CONCLUSION

The results of theoretical and finite element simulations of the HDD process showed that theoretical tearing pressure is always higher than tearing pressure obtained by finite element simulation.

REFERENCES

Dachang, K., C. Yu and X. Yongchao, 2005. Hydromechanical deep drawing of superalloy cups. J. Mater. Process. Technol., 166: 243-246.

Hama, T., T. Hatakeyama, M. Asakawa, H. Amino, A. Makinouchi, H. Fujimoto and H. Takuda, 2007. Finite-element simulation of the elliptical cup deep drawing process by sheet hydroforming. Finite Elements Anal. Des., 43: 234-246.

Kandil, A., 2003. An experimental study of hydroforming deep drawing. J. Mater. Process. Technol., 134: 70-80.

Khandeparkar, T. and M. Liewald, 2008. Hydromechanical deep drawing of cups with stepped geometries. J. Mater. Process. Technol., 202: 246-254.

Lang, L., J. Danckert and K. Nielsen, 2005a. Investigation into hydrodynamic deep drawing assisted by radial pressure Part II. Numerical analysis of the drawing mechanism and the process parameters. J. Mater. Process. Technol., 166: 150-161.

Lang, L., J. Danckert, K. Nielsen and X. Zhou, 2005b. Investigation into the forming of a complex cup locally constrained by a round die based on an innovative hydromechanical deep drawing method. J. Mater. Proess. Technol., 167: 191-200.

Parsa, M.H. and P. Darbandi, 2008. Experimental and numerical analyses of sheet hydroforming process for production of an automobile body part. J. Mater. Process. Technol., 198: 381-390.

Soo-Ik, O., J. Byung-Hee, K. Hyun-Yong and Y. Jae-Bong, 2006. Applications of hydroforming processes to automobile parts. J. Mater. Process. Technol., 174: 42-55.

Sy-wei, L., H. Tze-Chi and W.R.D. Wilson, 1993. An analysis of the hemispherical-punch hydroforming process. J. Mater. Process. Technol., 37: 225-239.

Thiruvarudchelvan, S. and M.J. Tan, 2006. A note on fluid-pressure-assisted deep drawing processes. J. Mater. Process. Technol., 172: 174-181.

Tirosh, J. and A. Hazut, 1989. The hydrodynamic deep-drawing process for blanks of non-uniform thickness. Int. J. Mech. Sci., 31: 121-130.

Wu, J., R. Balendra and Y. Qin, 2004. A study on the forming limits of the hydromechanical deep drawing of components with stepped geometries. J. Mater. Process. Technol., 145: 242-246.

Yossifon, S. and J. Tirosh, 1985. Rupture instability in hydroforming deep-drawing process. Int. J. Mech. Sci., 27: 559-570.

Yossifon, S. and J. Tirosh, 1991. On the dimensional accuracy of deep drawing products by hydroforming processes. Int. J. Mech. Sci., 33: 279-295.

Zhang, S.H., M.R. Jensen, J. Danckert, K.B. Nielsen, D.C. Kang and L.H. Lang, 2000. Analysis of the hydromechanical deep drawing of cylindrical cups. J. Mater. Process. Technol., 103: 367-373.